New sites of two Cr^{3+} EPR centres in $KTiOPO_4$ single crystals

1995 J. Phys.: Condens. Matter 7 667

(http://iopscience.iop.org/0953-8984/7/3/020)

J. Phys.: Condens. Matter 7 (1995) 667–674. Printed in the UK

New sites of two Cr^{3+} EPR centres in $KTiOPO_4$ single crystals

Sang Won Ahn†, Sung Ho Choh† and Jung Nam Kim‡
† Department of Physics, Korea University, Seoul 136-701, Korea
‡ Department of Physics, Pusan National University, Pusan 609-735, Korea

Received 24 August 1994, in final form 12 October 1994

Abstract. EPR spectra of Cr^{3+} ions in single crystals of $KTiOPO_4$ (KTP), synthesized by the flux method, have been investigated at room temperature by employing a Bruker Q-band spectrometer. From the angular dependence of the EPR pattern measured in the *ab*, *bc*, and *ca* planes, we have identified two Cr^{3+} centres, named A and B, which have been previously analysed by other investigators. In this study, we have newly identified four magnetically inequivalent Cr^{3+} sites for both A and B. For the four sites of both A and B, the direction cosines of the principal axes of the $\tilde{g}$ as well as the second-order zero-field-splitting (ZFS) tensors are found to be given by the relationship *lmn*, $\bar{l}mn$, $l\bar{m}n$, and $lm\bar{n}$. Using the site-rotation matrices obtained by this relationship, we calculated two sets of all spin-Hamiltonian parameters that simultaneously fitted four sites for both A and B. It is also verified that observed orientations of the principal axes for all Cr^{3+} sites are consistent with the crystallographic symmetry of KTP. Two possible origins of the centres A and B are proposed: each centre may be due to Cr^{3+} ions at crystallographically equivalent Ti sites, either Ti(1) or Ti(2), with different charge compensators, or at two different Ti sites, Ti(1) and Ti(2), without charge compensators.

1. Introduction

Potassium titanium phosphate $KTiOPO_4$ (KTP) is a relatively new, efficient, and promising non-linear optical material [1]. In particular, KTP is considered as a most suitable material for frequency doubling of laser radiation because of its high non-linear optical coefficient and high laser-damage threshold. The crystal structure of KTP is orthorhombic and belongs to the point group $mm2$ (space group $Pna2_1$) with eight formular units per unit cell [2]. Lattice constants for KTP are $a = 12.814$, $b = 6.404$, and $c = 10.616$ Å at room temperature. The structure exhibits two crystallographically different Ti sites: Ti(1) and Ti(2). Therefore, there are four chemically equivalent Ti sites per unit cell. Both sites lie in slightly distorted O octahedra with local site symmetry C_1, and exhibit approximately the same bond lengths and angle within the respective TiO_6 complex.

The Cr^{3+} EPR in KTP has been initiated by Hasanova *et al* [3]. Gaite *et al* [4] identified two Cr^{3+} centres, named A and B, which correspond to I and II=VI, respectively, reported by Hasanova *et al* [3]. It has been reported that the A and B centres are due to Cr^{3+} ions at the crystallographically equivalent Ti positions, either Ti(1) or Ti(2) with different charge compensators. However, there are four magnetically inequivalent Ti(1) and Ti(2) sites in KTP, and the study related to these sites has not been carried out yet.

In the present work, we have newly identified four magnetically inequivalent Cr^{3+} sites for the centres A and B. For four sites of both A and B, the principal values of the $\tilde{g}$ and the second-order zero-field-splitting (ZFS) tensors, and the orientations of their principal axes, were determined. Using the site-rotation matrices obtained by the symmetry relationship among four sites, we calculated two sets of all spin-Hamiltonian parameters

0953-8984/95/030667+08$19.50

that simultaneously fitted four sites for both A and B. Comparing the orientations of the principal axes with the point group *mm*2 of KTP, we were able to identify the relative sites of the Cr^{3+} ions. Two possible origins of the A and B centres are also discussed.

2. Experimental procedure

KTP crystals were synthesized by the flux method. The chemical $K_6P_4O_{13}$ known [5, 6] as a particularly suitable flux for growing KTP single crystals, was obtained by the following process [7]:

$$2K_2HPO_4 + 2KH_2PO_4 \xrightarrow{300^{\circ}C} K_6P_4O_{13} + 3H_2O. \tag{1}$$

A sample of $3.0 \times 2.1 \times 1.5$ mm^3 along the *a*, *b*, and *c* axis, respectively, was cut from the crystal. The Cr^{3+} ions in grown crystals were present as an impurity in the material and identified by comparing EPR results of Gaite *et al* [4]. EPR measurements of Cr^{3+} centres in KTP have been carried out at room temperature by employing a Bruker Q-band spectrometer (ESP 300 series) with 100 kHz modulation at the Seoul Branch of Korea Basic Science Centre. The microwave frequency was calibrated using the resonance magnetic field of DPPH, where the magnetic field scale at 1.2000 T was calibrated using a Bruker NMR Gaussmeter. These frequencies during the measurements were kept in the range of 0.001 GHz at 33.855, 33.996, and 34.023 GHz in the *ab*, *bc*, and *ca* plane, respectively.

Since the angular dependence of Cr^{3+} spectra varied up to 50 mT/deg and the EPR signals were split by small deviations of the crystal setting from the exact orientation, it was very important to establish a precise crystal orientation in order to study the accurate angular dependence. The crystal oriented by the x-ray Laue method was fixed to its holder, and mounted inside the cylindrical cavity in such a way that each crystallographic plane was perpendicular to the rotation axis of the magnet by adjusting the sample to achieve superposition of appropriately related EPR lines. Reiterating these procedures, we established the crystal orientations within $\pm 0.05^{\circ}$ for all rotation measurements. EPR spectra were recorded by varing the orientations of the external magnetic field in three mutually perpendicular crystallographic planes with θ and ϕ ranging from zero to 180° at 4° intervals, where the polar angle θ and the azimuthal angle ϕ in spherical polar coordinates are measured from the *c* and the *a* axis, respectively.

From the angular dependence of the EPR spectra measured in the *ab*, *bc*, and *ca* planes, three allowed transitions ($\Delta M_s = \pm 1$) between spin states were clearly identified in all crystallographic planes: $|3/2\rangle \leftrightarrow |1/2\rangle$, $|1/2\rangle \leftrightarrow |-1/2\rangle$ and $|-1/2\rangle \leftrightarrow |-3/2\rangle$. We also found two forbidden transitions ($\Delta M_s = \pm 2$): $|3/2\rangle \leftrightarrow |-1/2\rangle$ and $|1/2\rangle \leftrightarrow |-3/2\rangle$. For any arbitrary orientation of the magnetic field with respect to the crystallographic axes, eight sets of fine structures were observed. The eight sets can be divided into two groups denoted as A and B, which are related to symmetries of the Cr^{3+} ion sites. Each group contains four sets of fine structures, which arise from chemically equivalent but magnetically inequivalent Cr^{3+} ion sites. However, when the magnetic field was aligned along one of the three crystallographic planes, two sets of fine structures were recorded. These sets merged into only one when the magnetic field was oriented along a crystallographic axis.

3. Results and discussion

EPR spectra of Cr^{3+} ($S = 3/2$) are described by the general spin Hamiltonian up to second order as previously reported [4] for which no particular symmetry of the spin Hamiltonian is expected:

$$H = \sum_{ij} \mu_B B_i g_{ij} S_j + \sum_{m=-2}^{2} B_2^m O_2^m \tag{2}$$

where μ_B is the Bohr magneton, g_{ij} ($i, j = X, Y, Z$) the component of the **g** tensor and O_n^m the extended Stevens operators. From the angular dependence of EPR spectra measured in the *ab*, *bc*, and *ca* planes, respectively, we have identified two Cr^{3+} centres, which are equivalent to the A and B centres previously reported by Gaite *et al* [4]. We also have newly identified four magnetically different Cr^{3+} sites for both A and B, which arise from the symmetry of the point group *mm*2 of KTP. These new sites have been named SA1, SA2, SA3, and SA4 belonging to centre A, and SB1, SB2, SB3, and SB4 belonging to centre B.

For all Cr^{3+} sites, the 11 parameters of equation (1) are calculated by employing a computer program. In order to compare the results from the EPR program with other experimental data [4], the D_{ij} values are converted to the Stevens operator notation [8] using the relations [9]. For four sites belonging to each centre, the direction cosines of the principal axes of the **g** as well as the second-order ZFS tensors are found to be given by the relationship lmn, $\bar{l}mn$, $l\bar{m}n$, and $lm\bar{n}$. The site-rotation matrices, which transform all symmetry-related sites into a reference site, could be found by this relationship. Using this matrix set for each centre, we calculated two sets of the general spin-Hamiltonian parameters that simultaneously fitted the data of four sites for both A and B. The values of g_{ij} and of the second-order ZFS parameters for the sites SA1 and SB1 are listed in table 1. These parameters are given in the crystallographic axis system defined as $X = a$, $Y = b$, and $Z = c$. The standard deviations between the experimental and calculated magnetic transitions are 1.3 mT and 1.5 mT for A and B, respectively.

Table 1. Cr^{3+} spin-Hamiltonian parameters of the sites SA1 and SB1 belonging to the centres A and B respectively in the X, Y, Z crystallographic axis system. The estimated statistical uncertainties in the last significant figures are represented in parentheses.

	A (site SA1)	B (site SB1)
ij	Matrix components g_{ij}	
XX	1.963 79(15)	1.972 61(16)
YY	1.975 52(18)	1.967 49(17)
ZZ	1.971 43(19)	1.972 61(17)
XY	0.000 63(19)	−0.000 66(17)
XZ	−0.000 68(17)	−0.001 56(18)
YZ	−0.000 93(23)	0.000 73(17)
m	Second-order ZFS parameters B_2^m (cm^{-1})	
0	−0.116 60(3)	−0.085 77(2)
1	0.005 85(11)	0.215 58(9)
−1	−0.133 99(11)	−0.085 25(9)
2	0.210 50(4)	−0.171 81(3)
−2	−0.057 81(5)	0.071 48(4)

Table 2. Principal values of the **g** tensors and orientations of their principal axes x', y', z' with respect to the X, Y, Z crystallographic axis system for Cr^{3+} sites belonging to the centres A and B.

	A		B	
Components	Principal values of **g** tensors[a]			
$g_{x'}$	1.975 77(18)		1.974 10(21)	
$g_{y'}$	1.971 26(21)		1.970 82(20)	
$g_{z'}$	1.963 71(15)		1.967 35(17)	
	Orientations (°) of the principal values[a,b]			
	θ	ϕ	θ	ϕ
	SA1		SB1	
Ox'	102.7(2.7)	86.3(0.9)	130.7(2.1)	−11.1(1.9)
Oy'	13.5(2.6)	107.4(6.5)	138.5(2.2)	−177.1(4.1)
Oz'	94.7(1.3)	177.3(0.9)	83.0(2.3)	−95.1(2.2)
	SA2		SB2	
Ox'	102.7	93.8	49.3	11.1
Oy'	166.5	−107.4	138.5	−2.9
Oz'	85.3	−177.3	83.0	−84.9
	SA3		SB3	
Ox'	77.4	93.8	130.7	11.1
Oy'	166.5	72.6	138.5	177.1
Oz'	94.7	−177.3	97.0	−84.9
	SA4		SB4	
Ox'	77.4	86.3	49.3	−11.1
Oy'	166.5	107.4	138.5	2.9
Oz'	94.7	−2.7	97.0	−95.1

[a] The estimated statistical uncertainties in the last significant figures are represented in parentheses.

[b] The ranges of θ and ϕ are restricted to $0 \leqslant \theta < \pi$ and $-\pi \leqslant \phi < \pi$, respectively.

For eight sites, the principal values of the **g** tensors and the orientations of their principal axes x', y', z' with respect to the crystallographic axis system are summarized in table 2, where the axes x', y', z' are taken in the order of their magnitudes: $g_{x'} > g_{y'} \geqslant g_{z'}$. The principal values of the second-order ZFS tensors, and the orientations of their principal axes x, y, z with respect to the crystallographic axis system, are listed in table 3 together with the values reported by Gaite *et al* [4] for comparison. We chose the principal axes to follow the general rule $|B_2^0| \geqslant |B_2^2|$ and two parameters having the same sign. Four Cr^{3+} sites corresponding to each of A and B have identical principal values of the **g** and the second-order ZFS tensors within the experimental uncertainty, but different orientations of their principal axes, respectively. The site SA3 (SB4) corresponds directly to the centre A (B) reported by Gaite *et al* [4], where the orientation of their principal axis Oz of the second-order ZFS tensors is perpendicular to the xy plane that is made up of the other principal axes, but is in the left-handed instead of the right-handed coordinate system x, y, z.

In order to demonstrate the confidence of the determined parameters, the calculated

Table 3. Principal values of the second-order ZFS tensors and orientations of their principal axes x, y, z with respect to the X, Y, Z crystallographic axis system for Cr^{3+} sites corresponding to the centres A and B. The data of Gaite *et al* [4] are included for comparison.

	Present work			
	A		B	
	Principal values of the second-order ZFS tensors[a]			
B_2^0 (cm^{-1})	0.167 57(3)		0.136 45(3)	
B_2^2 (cm^{-1})	0.093 24(2)		0.119 49(3)	
	Orientations (°) of the principal axes of the second-order ZFS tensors[b]			
	θ	ϕ	θ	ϕ
	SA1		SB1	
Ox	112.52	81.63	53.88	−8.30
Oy	157.45	−94.93	143.72	−14.36
Oz	91.22	172.14	92.89	79.59
	SA2		SB2	
Ox	112.52	98.37	126.12	8.30
Oy	157.45	−85.07	143.72	−165.64
Oz	88.78	−172.14	92.89	100.41
	SA3		SB3	
Ox	67.48	98.37	53.88	8.30
Oy	157.45	94.93	36.28	−165.64
Oz	91.21	−172.14	92.89	−79.59
	SA4		SB4	
Ox	67.48	81.63	126.12	−8.30
Oy	157.45	85.07	36.28	−14.36
Oz	88.78	172.14	92.89	−100.41
	Gaite *et al*			
	A		B	
B_2^0 (cm^{-1})	0.1686		0.1373	
B_2^2 (cm^{-1})	0.0939		0.1197	
Ox	67.5	98.4	126.1	−8.3
Oy	157.4	94.9	36.3	−14.4
Oz	88.8	7.9	87.1	79.5

[a] The numbers in parentheses represent the estimated statistical uncertainties in the last significant figures.

[b] The ranges of θ and ϕ are restricted to $0 \leqslant \theta < \pi$ and $-\pi \leqslant \phi < \pi$, respectively, where the estimated maximum uncertainties in the angle are $\pm 0.01°$ for all sites.

rotation patterns of the centres A and B in the ab, bc and ca planes are displayed in figure 1 together with experimental data. Four Cr^{3+} sites for each centre are differently degenerated into two pairs in three crystallographic planes, respectively. The degenerated pairs are as follows. The SA1 (SB1) and SA4 (SB4), indicated by closed circles, and

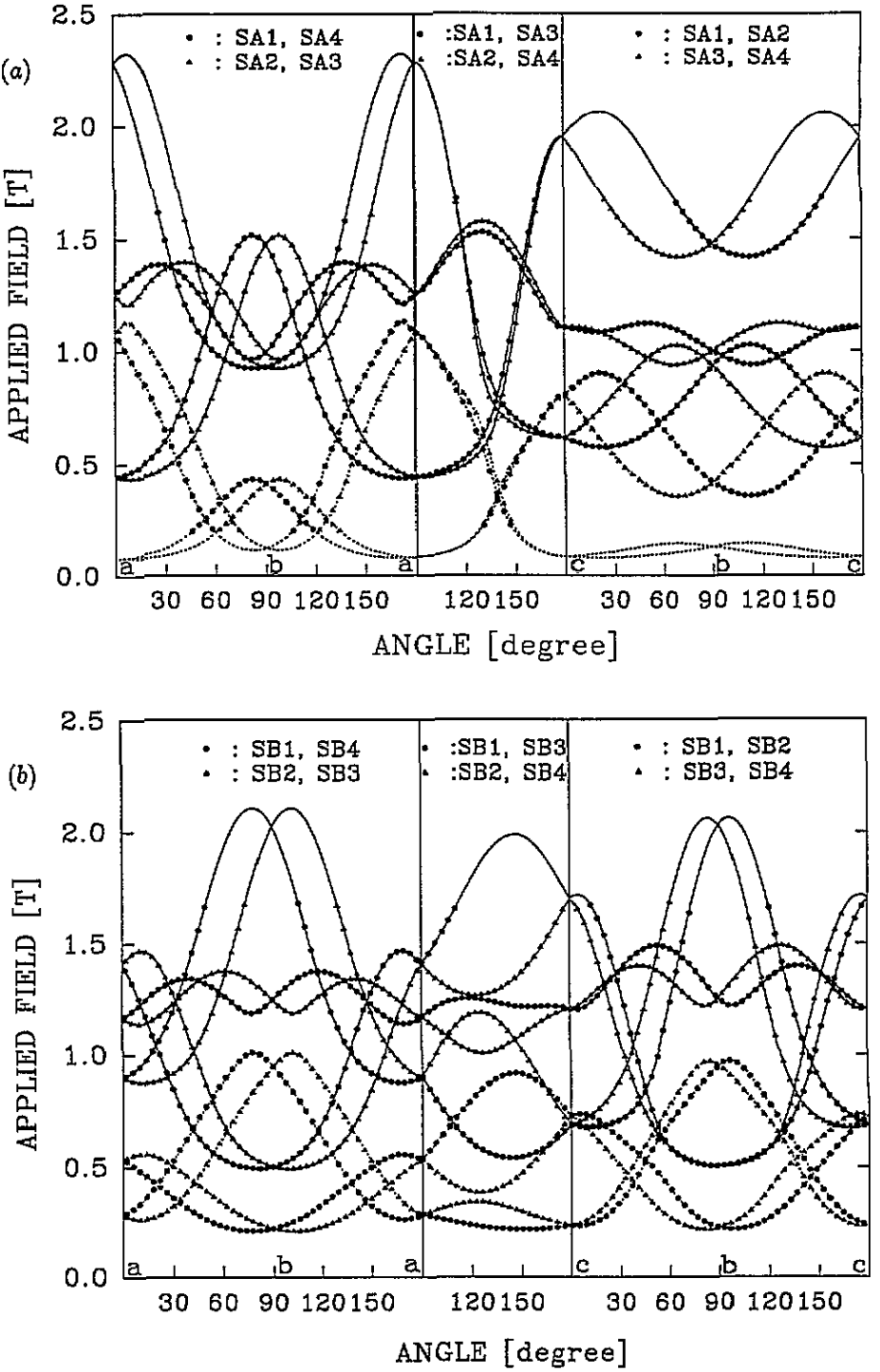

Figure 1. The angular dependence of the Cr^{3+} spectra in KTP in the *ab*, *bc*, and *ca* planes, at 33.885, 33.996, and 34.023 ± 0.001 GHz, respectively: (a) for the A centre; (b) for the B centre. The experimental points are represented by closed circles and triangles, and calculations by full lines for the allowed transitions and by dotted lines for the forbidden transitions.

SA2 (SB2) and SA3 (SB3), by closed triangles, are degenerated respectively into one in the *ab* plane. The SA1 (SB1) and SA2 (SB2) indicated by closed circles and SA3 (SB3) and SA4 (SB4) by closed triangles in the *bc* plane, and the SA1 (SB1) and SA3 (SB3) by closed circles and SA2 (SB2) and SA4 (SB4) by closed triangles in the *ca* plane, are each degenerated into one. The non-degenerated pair has a mirror symmetry to each other about the *a*, *b*, and *c* axis in each crystallographic plane.

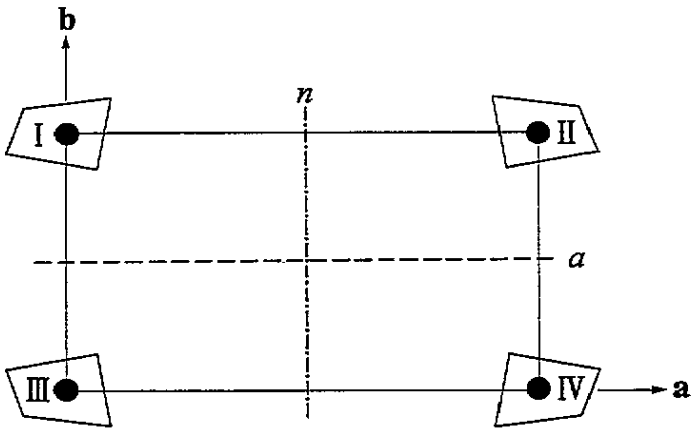

Figure 2. The symmetry relationship among four crystallographically equivalent Ti^{4+} positions in KTP.

The point-symmetry relationship among the Ti^{4+} positions in KTP is described in figure 2. When the magnetic field is aligned along one of the three crystallographic planes, the distinction of lattice translations as part of the symmetry operations in the space group $Pna2_1$ can be ignored; i.e. the twofold screw axis **c** can be considered as a twofold rotation axis, and glide planes *a* and *n* as mirror planes. Therefore, if the magnetic field is aligned along the *a*, *b*, and *c* axis, then the resonance field will be identical for all Ti^{4+} positions. When the magnetic field is along the *ab* plane, the resonance fields are identical for I and IV, and II and III positions, respectively. The resonance fields are respectively identical for I and II, and III and IV in the *bc* plane, likewise I and III, and II and IV in the *ca* plane, respectively. Therefore, the sites SA1, SA2, SA3, and SA4 belonging to the A centre correspond to I, II, III, and IV positions, respectively. In the same way, the SB1, SB2, SB3, and SB4 sites belonging to centre B can be correlated with the other set of four Ti^{4+} positions that have the relationship shown in figure 2.

It is possible to partially substitute for the Ti^{4+} ion in TiO_6 octahedra by a Cr^{3+} ion of similar ionic radius, but with a monovalent charge compensator. Therefore, there are two possible origins of the centres A and B: each centre may be due to Cr^{3+} ions at the crystallographically equivalent Ti sites, either Ti(1) or Ti(2) with different charge compensators, or at two different Ti sites, Ti(1) and Ti(2) without charge compensators.

Acknowledgments

This work was supported by the Korea Science and Engineering Foundations through the Science Research Centre of Exellence Program (1994–1997). The computer program 'EPR

version 4.4′ (D G McGavin, M Y Mombourquette and J A Weil, Department of Chemistry, University of Saskatchewan, Canada) was employed.

References

[1] Zumsteg F C, Bierlein J D and Gier T E 1976 *J. Appl. Phys.* 47 4980
[2] Tordjman I, Masse R and Guitel J C 1974 *Z. Kristallogr.* **139** 103
[3] Hasanova N M, Nizamutdinov N M, Izugzon A S, Bulka G R, Vinokurov V M, Pavlova N I and Rez I S 1988 *Physics of Minerals and Synthetic Crystals* (in Russian) (Kazanskogo University Press) p 87
[4] Gaite J M, Stenger J F, Dusausoy Y, Marnier G and Rager H 1991 *J. Phys.: Condens. Matter* **3** 7877
[5] Bordui P F, Jacco J C, Loiacono G M, Stolzenberger R A and Zola J J 1987 *J. Cryst. Growth* **84** 403
[6] Bolt R J, De Hass H, Sebastian M T and Klapper H 1991 *J. Cryst. Growth* **110** 587
[7] Choi B C, Kim J B, Yun S I and Kim J N 1993 *Korean Appl. Phys.* **6** 27
[8] Rudowicz C 1987 *Magn. Res. Rev.* **13** 1
[9] McGavin D G 1987 *J. Magn. Res.* **74** 19